

SPMTrack: Spatio-Temporal Parameter-Efficient Fine-Tuning with Mixture of Experts for Scalable Visual Tracking

Wenrui Cai¹, Qingjie Liu^{1,2,3,*}, Yunhong Wang^{1,3}

¹State Key Laboratory of Virtual Reality Technology and Systems, Beihang University, Beijing, China

²Zhongguancun Laboratory, Beijing, China

³Hangzhou Innovation Institute, Beihang University, Hangzhou, China

{wenrui.cai, qingjie.liu, yhwang}@buaa.edu.cn

Abstract

Most state-of-the-art trackers adopt one-stream paradigm, using a single Vision Transformer for joint feature extraction and relation modeling of template and search region images. However, relation modeling between different image patches exhibits significant variations. For instance, background regions dominated by target-irrelevant information require reduced attention allocation, while foreground, particularly boundary areas, need to be emphasized. A single model may not effectively handle all kinds of relation modeling simultaneously. In this paper, we propose a novel tracker called *SPMTrack* based on mixture-of-experts tailored for visual tracking task (TMoE), combining the capability of multiple experts to handle diverse relation modeling more flexibly. Benefiting from TMoE, we extend relation modeling from image pairs to spatio-temporal context, further improving tracking accuracy with minimal increase in model parameters. Moreover, we employ TMoE as a parameter-efficient fine-tuning method, substantially reducing trainable parameters, which enables us to train *SPMTrack* of varying scales efficiently and preserve the generalization ability of pretrained models to achieve superior performance. We conduct experiments on seven datasets, and experimental results demonstrate that our method significantly outperforms current state-of-the-art trackers. The source code is available at <https://github.com/WenRuiCai/SPMTrack>.

1. Introduction

Visual tracking aims to predict the location of a target throughout subsequent frames of a video, given the initial state in the first frame template. Currently, most state-of-the-art trackers adopt a Transformer-based [51] one-stream

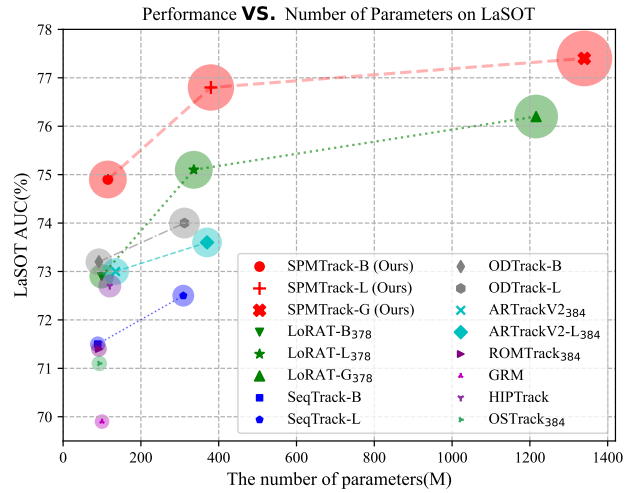


Figure 1. Comparison of LaSOT AUC and model parameter count across different trackers. Larger loop indicates better performance.

paradigm [3, 5, 10, 37, 57, 64, 69], utilizing a single Vision Transformer [12] backbone that accepts both the template and the search region image as input, and employs self-attention to perform image feature extraction and template-search region relation modeling simultaneously.

However, not all relation modeling between image patches benefits tracking performance. Prior studies [4, 20, 63, 64] have demonstrated that the abundance of background patches in the search region deteriorates the discriminative power of the foreground features, and single vanilla attention has limited capability in suppressing undesirable foreground-background interactions. Meanwhile, there are also some kinds of relation modeling that demonstrate positive effects on tracking performance [17, 19]. For instance, enhancing attention to target boundary regions can improve tracking performance [17], especially in challenging scenarios such as motion blur, partial occlusion, and deformation.

To address various relation modeling, numerous meth-

*Corresponding author.

ods propose specific designs, including background filtering to reduce target-irrelevant information [3, 64], customizing different interaction modules for tokens belonging to different categories [4, 20], and attention score adjustment based on foreground-background weights of each token [63]. However, existing methods can only handle one or a few predefined types of relation modeling, and the hand-crafted strategies inherently lack adaptability. Furthermore, there may exist many latent relationships that further complicate the specialized design. These limitations motivate our question: *How to design a tracker to adaptively process various relation modeling between image patches?*

Inspired by mixture of experts (MoE) [1, 11, 13, 31, 46] in natural language processing, in this paper, we address the question by proposing **SPMTrack**, a novel tracker based on TMoE, a specialized mixture of experts module for visual tracking task. Similar to MoE, TMoE handles diverse relation modeling through adaptive weighted combinations of multiple experts. However, unlike traditional MoE that is exclusively applied to feed-forward network (FFN) layers, TMoE is simultaneously applied to the linear layers within both the attention layers and the FFN layers. This finer-grained application enables TMoE to achieve more diverse expert combinations, thereby enhancing the capability of various relation modeling. Moreover, differing from traditional MoE that uses FFNs as experts, all the experts in TMoE are linear layers and designed with a lightweight and efficient structure to ensure overall efficiency. Furthermore, we employ TMoE as a parameter-efficient fine-tuning method, which enables us to train SPMTrack of larger scales. In SPMTrack, only a subset of experts and the router within TMoE, along with the prediction head need to be trained, which substantially reduces the trainable parameters while preserving the generalization capability of pretrained models. Notably, our method reduces the number of trainable parameters by nearly 80% compared to [2], while demonstrates better performance.

Benefiting from the powerful capability of TMoE in handling diverse relation modeling, unlike previous one-stream trackers that only perform relation modeling between template-search region pairs, we extend SPMTrack to incorporate multi-frame spatio-temporal context modeling, which further enhances the performance of SPMTrack with minimal additional parameters. We evaluated the performance of our method on seven datasets, and the experimental results demonstrate that SPMTrack achieves state-of-the-art performance across multiple datasets including LaSOT [14], GOT-10K [26], TrackingNet [43] and TNL2K [54]. Through extensive experiments with models of varying scales, as shown in Figure 1, Table 1 and Table 2, with ViT-B [12] as backbone and less than 30% of parameters need to be trained, SPMTrack-B achieves or even surpasses the best performance of previous trackers utilizing ViT-L.

The main contributions of this paper can be summarized as: **(1)** We propose TMoE, a mixture of experts module tailored for visual tracking. TMoE enhances the capability to handle various relation modeling and can be used as a method of parameter-efficient fine-tuning. **(2)** Based on TMoE, we propose SPMTrack, a novel tracker that can effectively integrate spatio-temporal context for visual tracking. **(3)** Experimental results demonstrate that SPMTrack achieves state-of-the-art performance across multiple datasets. We trained SPMTrack of varying scales, and our method with ViT-B as backbone can achieve or even surpass current trackers using ViT-L.

2. Related Work

2.1. One-Stream Trackers

One-stream trackers employ a single Vision Transformer [12] as backbone, simultaneously performing feature extraction and relation modeling at each layer [5, 10, 60, 64]. Many efforts focus on incorporating historical context. TATrack [23] and ODTrack [69] propose architectures capable of processing multiple frames, while HIPTrack [3] introduces historical target features through prompt learning. SeqTrack [6], ARTrack[56], and ARTrackV2 [2] achieve more precise predictions by incorporating multiple historical target position. Other works try to improve conventional self-attention to handle different relation modeling. OSTRack [64] progressively filters background regions to reduce foreground-background relation modeling, GRM [20] and ROMTrack [4] categorizes image tokens and constrains relation modeling between specific categories, F-BDMTrack [63] adjusts the attention score by calculating the foreground-background weights of tokens. But these methods can only handle specific relation modeling and rely on manually designed strategies.

2.2. Mixture of Experts

Mixture-of-experts (MoE) [1, 13, 31] are widely applied in large language models [9, 11, 15, 40, 46, 58], where each expert focuses on specific aspects of the data or particular tasks [53]. By performing an adaptive weighted sum over multiple experts, MoE can better capture complex patterns and relationships within the input data. MoE also has applications in computer vision [8, 48, 65]. However, there is few dedicated exploration of MoE in visual tracking. MoETrack [49] employs multiple prediction heads as experts in the field of RGB-T tracking, which is rather far-fetched and deviates from the general practice of embedding MoE within Transformer layers. In the field of RGB-E tracking, eMoE-Tracker [7] inserts multiple experts between Transformer layers, which more closely resembles an adapter architecture [24] and contrasts with MoE implementations where experts are embedded within Transformer layers.

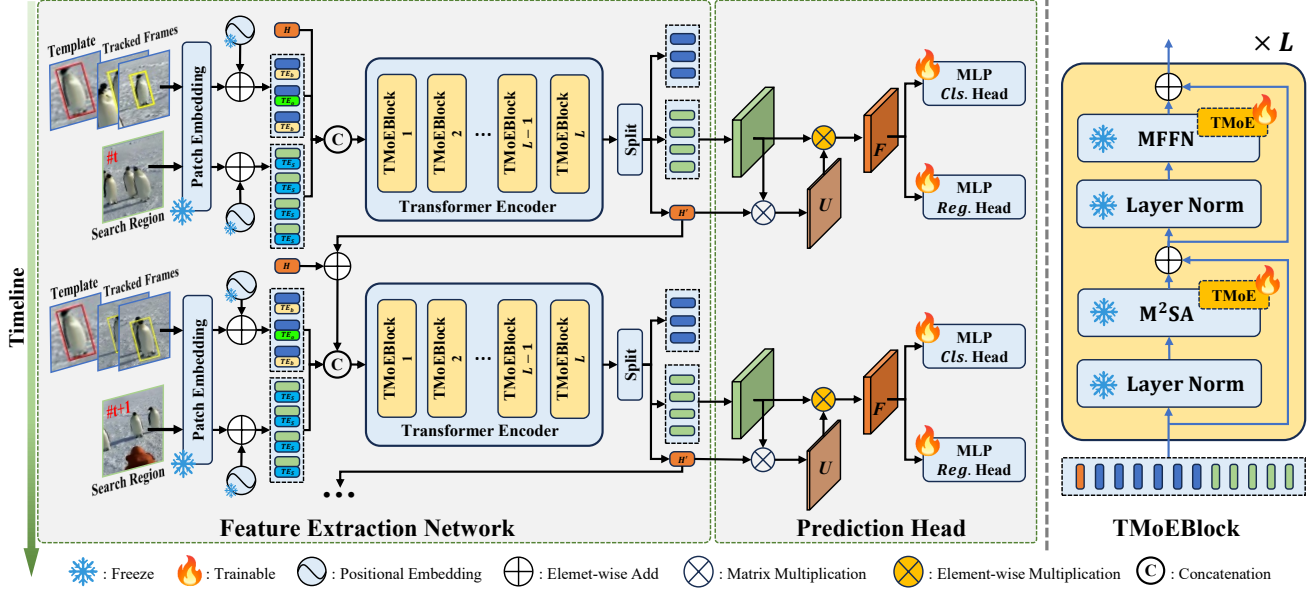


Figure 2. Overview of SPMTrack that consists of a feature extraction network and a prediction head. The main body of the feature extraction network is a Transformer encoder composed of multiple TMoEBlocks. The structure of TMoEBlock is shown on the right side.

2.3. Parameter-efficient Fine-tuning

Parameter-efficient fine-tuning aims to reduce computational costs and retain the general knowledge of the pretrained model by freezing most parameters and fine-tuning only a small subset of parameters. Common parameter-efficient fine-tuning approaches include adapter-based methods [18, 24, 45], prompt-based methods [32, 35, 55, 70] and low-rank adaptation methods [25, 50]. In visual tracking, HIPTrack [3] incorporates historical target features as prompts, while LoRAT [37] employs low-rank adaptation for efficient training. And our method maintains flexibility in diverse relation modeling while reducing trainable parameters by fine-tuning TMoE.

3. Method

3.1. Overall Architecture

As illustrated in Figure 2, we propose SPMTrack, a novel tracker that integrates multi-frame spatio-temporal context and employs TMoE for parameter-efficient fine-tuning. The overall architecture follows the one-stream paradigm, consisting of a Feature Extraction Network based on a Vision Transformer [12] as backbone, and a prediction head.

Feature Extraction Network. The feature extraction network is denoted as Φ . The main body of the feature extraction network is a Transformer encoder that utilizes TMoEBlock as its primary component, which is designed based on TMoE. The architecture of TMoEBlock is illustrated in the right panel of Figure 2, and details will be introduced in Section 3.2. The encoder simultaneously per-

forms feature extraction and relation modeling for input images. We extend the input from one single template $Z \in \mathbb{R}^{H_z \times W_z \times 3}$ that is commonly used in one-stream trackers to the video sequence $\{Z_1, \dots, Z_N | Z_i \in \mathbb{R}^{H_z \times W_z \times 3}\}$ as reference frames. The reference frames contain the first frame template and the selected tracked historical frames, with a total of N frames. The feature extraction network uses patch embedding to partition each input image into patches of size $M \times M$, map all patches into tokens by a convolutional layer, and obtain the reference token sequence of each image $T_i \in \mathbb{R}^{N_T \times d}$, where d denotes the hidden dimension of Transformer encoder and $N_T = \frac{H_z W_z}{M^2}$ represents the number of tokens corresponding to each image. Similarly, for the search region $S \in \mathbb{R}^{H_s \times W_s \times 3}$, we can also obtain the token sequence $X \in \mathbb{R}^{N_x \times d}$. All tokens are added with positional embedding and a learnable token type embedding [37]. Inspired by [36, 69], we additionally introduce a target state token $H \in \mathbb{R}^{1 \times d}$ that is learnable as well and propagates over time. All tokens are concatenated and fed into the Transformer encoder. The process can be formulated as:

$$\begin{aligned}
 T_i^j &= \begin{cases} T_i^j + PE_j + TE_o, & \text{if token } (i, j) \text{ in bbox} \\ T_i^j + PE_j + TE_b, & \text{otherwise} \end{cases} \\
 X^j &= X^j + PE_j + TE_S \\
 I &= \text{Concat}(H, T_1, \dots, T_N, X)
 \end{aligned} \tag{1}$$

where T_i^j represents the j^{th} token in T_i , PE_j represents positional embedding of the j^{th} token, similarly for X^j . TE_o , TE_b and TE_S represents the learnable type embeddings of the foreground region tokens, background region

tokens in reference frames and the search region tokens, respectively. \mathbf{I} denotes the input to the Transformer encoder.

Subsequently, the Transformer encoder processes all tokens and produces an output $\mathbf{O} \in \mathbb{R}^{(1+N \times N_T + N_x) \times d}$. The output tokens $\mathbf{X}' \in \mathbb{R}^{N_x \times d}$ corresponding to search region and the output $\mathbf{H}' \in \mathbb{R}^{1 \times d}$ from the target state token are fed into the prediction head for prediction. \mathbf{H}' will be added with the input target state token in the next tracking frame, which can be formulated as:

$$\mathbf{O} = \Phi(\mathbf{I}), [\mathbf{H}', \mathbf{T}'_1, \dots, \mathbf{T}'_N, \mathbf{X}'] = \text{Split}(\mathbf{O}) \quad (2)$$

Prediction Head. The input to the prediction head consists of the output target state token \mathbf{H}' and the output search region tokens \mathbf{X}' from the feature extraction network. Initially, the prediction head performs matrix multiplication between \mathbf{H}' and \mathbf{X}' to obtain the weight $\mathbf{U} \in \mathbb{R}^{N_x \times 1}$. As the target state token propagates over time, \mathbf{U} can re-weight and adjust current search region tokens based on the historical state of the target, thereby introducing more spatio-temporal tracking context. After element-wise multiplication of \mathbf{X}' with \mathbf{U} , the resulting data is reshaped into a feature map $\mathbf{F} \in \mathbb{R}^{\frac{H_s}{M} \times \frac{W_s}{M} \times d}$, which is then processed by a decoupled double-MLP head to perform target center classification and box regression, respectively. For fair comparison, the double-MLP head is identical to [37].

3.2. The Design of TMOEBlock

TMOEBlock serves as the primary component of the Transformer encoder in the feature extraction network. As illustrated in the right of Figure 2, TMOEBlock is built based on the standard vision Transformer block. However, unlike the standard ViT block, TMOEBlock applies TMOE module to both the multi-head self-attention (MSA) layer and the feed-forward network (FFN) layer, obtaining MoE-based MSA (M²SA) layer and MoE-based FFN (MFFN) layer. The finer-grained application of TMOE is capable to achieve more diverse combinations for various relation modeling. The processing of TMOEBlock can be formulated as:

$$\begin{aligned} \mathbf{O}'_l &= \text{M}^2\text{SA}(\text{LN}(\mathbf{O}_{l-1})) + \mathbf{O}_{l-1}, \quad l = 1, \dots, L \\ \mathbf{O}_l &= \text{MFFN}(\text{LN}(\mathbf{O}'_l)) + \mathbf{O}'_l, \quad l = 1, \dots, L \end{aligned} \quad (3)$$

where L denotes the total number of TMOEBlocks, \mathbf{O}_l represents the output of the l^{th} block in Transformer encoder. When $l = L$, \mathbf{O}_l is the output \mathbf{O} of the feature extraction network; when $l = 0$, it is the overall input \mathbf{I} . LN stands for the layer normalization operation.

MoE-based Multi-head Self-Attention (M²SA). M²SA not only replaces the standard three linear projection layers \mathbf{Q} , \mathbf{K} , \mathbf{V} in standard attention for the query, key, and value with TMOE modules but also replaces the output projection layer with TMOE module.

MoE-based Feed-Forward Network (MFFN). Conventional feed-forward network consists of two linear layer and

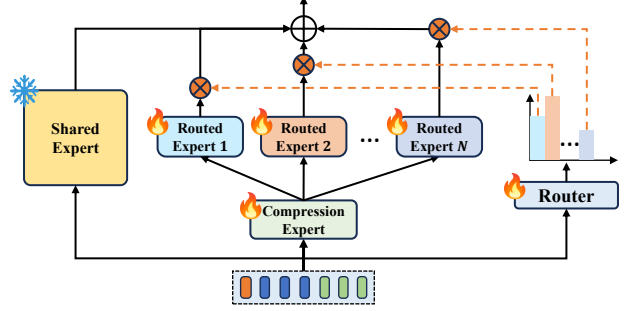


Figure 3. The structure of TMOE. The symbols maintain the same meaning with Figure 2.

activation function. MFFN replaces both linear layers in FFN with TMOE modules, while maintaining all other architectural configurations unchanged.

3.3. Mixture of Experts for Visual Tracking

In this section, we introduce TMOE, a mixture of experts module tailored for visual tracking task. As illustrated in Figure 3, TMOE consists of one shared expert, one router, one compression expert and N_e routed experts. In large language models, mixture of experts are commonly applied to replace FFN layers, and the experts comprising MoE are typically the same structure as FFN. However, TMOE is used to replace the linear layers in both self-attention and FFN, and the shared expert, the compression expert and the routed experts are all implemented as linear layers.

In TMOE, the shared expert directly copies weights from the corresponding linear layers in pretrained model and remains frozen during training. The rationale is that the original weights have been well-trained during the pre-training stage, and the shared expert needs to retain more general knowledge. In contrast, the compression experts, routed experts, and the router are all trainable.

Given a TMOE module replacing a linear layer with input dimension d and output dimension D , for each token $\mathbf{x} \in \mathbb{R}^d$, as shown in Figure 3, TMOE first computes the weights $\mathbf{W} \in \mathbb{R}^{N_e}$ of all routed experts based on the input \mathbf{x} , the weights are normalized by Softmax. After that, TMOE calculates the output $\mathbf{y}^s \in \mathbb{R}^D$ of the shared expert and the outputs $\mathbf{y}_i^e \in \mathbb{R}^D$ of all routed experts. In particular, instead of adopting the same structure as the shared expert, inspired by [50], we first employ a compression expert with a $d \times r$ linear transformation to reduce the input dimension from d to r and obtain the compressed result $\mathbf{y}^c \in \mathbb{R}^r$, where $r \ll d$ and $r \ll D$. Subsequently, all routed experts use the compressed input \mathbf{y}^c to produce their respective outputs $\mathbf{y}_i^e \in \mathbb{R}^D$. The process can be formally described as:

$$\begin{aligned} \mathbf{W} &= \text{Softmax}(\text{Router}(\mathbf{x})), \quad \mathbf{y}^s = \mathbf{E}^S(\mathbf{x}) \\ \mathbf{y}^c &= \mathbf{E}^C(\mathbf{x}), \quad \mathbf{y}_i^e = \mathbf{E}_i^R(\mathbf{y}^c) \quad i = 1, \dots, N_e \end{aligned} \quad (4)$$

where Router is also a linear layer that maps the input \mathbf{x}

to weights W , and E^S , E^C , and E_i^R denote the shared expert, compress expert, and i^{th} routed expert, respectively.

After obtaining the outputs of all experts, we compute a weighted sum of the outputs y_i^e from all routed expert based on W to obtain $y^e \in \mathbb{R}^D$, which means that the routed experts are densely activated in TMoE. Subsequently, y^e is added with the shared expert output y^s to get the final output $y \in \mathbb{R}^D$. The process can be formulated as follows:

$$y^e = \sum_{i=1}^{N_e} W_i y_i^e, \quad y = y^e + y^s \quad (5)$$

3.4. Loss Function

The outputs of the decoupled double-MLP prediction head are supervised using binary cross-entropy loss for target center classification and Generalized IoU loss [47] for bounding box regression, respectively. Both loss terms are assigned with the weighting coefficients set to 1.

4. Experiments

4.1. Implementation Details

Model settings. We provide three versions of SPMTrack: SPMTrack-B, SPMTrack-L, and SPMTrack-G, utilizing ViT-B [12], ViT-L [12], and ViT-G [44] as backbones respectively. All versions maintain a consistent patch size M of 14 and adopt the pretrained weights from DINOv2 [44]. The resolution of input images are the same across all versions, with reference frames of 196×196 and search region of 378×378 . A crop factor of 2 is applied to reference frames and 5 to search region. We set the number of reference frames N to 3 for spatio-temporal modeling. Each TMoE module incorporates 4 routed experts, where the input dimension of the routed experts r is set to 64. Other configurations and model information are shown in Table 1, where L is the number of TMoEBlocks, d denotes hidden dimension and N_h is the number of attention heads.

Table 1. Model configurations, parameter counts and computational amount across SPMTrack variants of different scales.

	SPMTrack-B	SPMTrack-L	SPMTrack-G
Backbone	$L = 12$ $d = 768$ $N_h = 12$	$L = 24$ $d = 1024$ $N_h = 16$	$L = 40$ $d = 1536$ $N_h = 24$
#Params (M)	115.3	379.6	1339.5
#Trainable Params (M)	29.2	75.9	204.0

Datasets. Following previous works [3, 37, 56, 64], we use LaSOT [14], TrackingNet [52], GOT-10K [26], and COCO [38] for training. When evaluating on GOT-10K *test* set, we strictly follow the protocol by training exclusively on GOT-10K *training* set. When evaluating on other datasets,

we jointly train on the *training* sets of all four datasets, randomly sampling from each dataset with equal probability. For video datasets, we sample 5 frames from one video with random frame intervals ranging from 1 to 200. The sampled frames are arranged either in forward or reverse order with equal probability, where the first 3 frames serve as reference frames and the remaining 2 as search frames. For COCO, we replicate each image 5 times to maintain consistency with the video frame sampling strategy.

Training and Optimization. Our method is implemented based on PyTorch 2.3.1 and trained on 8 NVIDIA A100 GPUs. We maintain a global batch size of 128 during training. When training exclusively on GOT-10K, we train for 100 epochs. When joint training on multiple datasets, we extend to 170 epochs. In each epoch, we sample 131,072 sequences. We employ AdamW [39] as optimizer with learning rate of 10^{-4} and weight decay of 0.1. The learning rate scheduler warms up over the initial 2 epochs from 10^{-7} to 10^{-4} and then follows a cosine schedule to 10^{-6} .

Inference. We use a total of 3 reference frames, including the annotated first frame template. When current search frame index $t \leq 3$, we use all available tracked frames as reference frames, if there are fewer than three frames, we repeat the template as necessary to reach the required number. When $t > 3$, we select two tracked frames as reference frames at indexes $\lfloor \frac{t}{3} \rfloor$ and $\lfloor \frac{2t}{3} \rfloor$. Following previous trackers [4, 64, 69], we apply a Hanning window penalty to the output response map of the classification head.

4.2. Comparisons with the State-of-the-Art

LaSOT [14] is a large-scale long-term tracking dataset with its *test* set containing 280 sequences. As shown in Table 2, SPMTrack-B significantly outperforms all trackers utilizing ViT-B as backbone. Our method also substantially surpasses LoRAT [37] that also employs parameter-efficient fine-tuning. Additionally, as shown in Figure 4, we evaluate tracker performance across various challenging scenarios in LaSOT. Our method surpasses previous trackers that also incorporate spatio-temporal context [2, 3, 6, 56, 61], while significantly outperforming ROMTrack [4] and GRM [20], which focus on optimizing relation modeling.

GOT-10K [26] contains 9,335 sequences for training and 180 sequences for testing. We follow the protocol that trackers are only allowed to be trained using GOT-10K *train* split. Our approach significantly outperforms LoRAT [37] with the same backbone. And our SPMTrack-B rivals the performance of the current state-of-the-art methods, while SPMTrack-L substantially surpasses all existing trackers.

TrackingNet [43] is a large-scale visual tracking dataset with a *test* set comprising 511 video sequences. Table 2 demonstrates that our method achieves state-of-the-art performance using only ViT-B as backbone, surpassing current trackers that utilize ViT-L or even ViT-G.

Table 2. State-of-the-art comparison on LaSOT, GOT-10k and TrackingNet. “**” denotes for trackers trained only with GOT-10k *train* split. The best three results are highlighted in **red**, **blue** and **bold**, respectively.

Method	Source	LaSOT			GOT-10k*			TrackingNet		
		AUC(%)	P_{Norm} (%)	P (%)	AO(%)	$SR_{0.5}$ (%)	$SR_{0.75}$ (%)	AUC(%)	P_{Norm} (%)	P (%)
SPMTrack-B	Ours	74.9	84.0	81.7	76.5	85.9	76.3	86.1	90.2	85.6
SPMTrack-L	Ours	76.8	85.9	84.0	80.0	89.4	79.9	86.9	91.0	87.2
SPMTrack-G	Ours	77.4	86.6	85.0	81.0	89.2	82.3	87.3	91.4	88.1
LoRAT-B ₃₇₈ [37]	ECCV24	72.9	81.9	79.1	73.7	82.6	72.9	84.2	88.4	83.0
LoRAT-L ₃₇₈ [37]	ECCV24	75.1	84.1	82.0	77.5	86.2	78.1	85.6	89.7	85.4
LoRAT-G ₃₇₈ [37]	ECCV24	76.2	85.3	83.5	78.9	87.8	80.7	86.0	90.2	86.1
AQATrack ₃₈₄ [61]	CVPR24	72.7	82.9	80.2	76.0	85.2	74.9	84.8	89.3	84.3
ARTrackV2-B ₃₈₄ [2]	CVPR24	73.0	82.0	79.6	77.5	86.0	75.5	85.7	89.8	85.5
ARTrackV2-L ₃₈₄ [2]	CVPR24	73.6	82.8	81.1	79.5	87.8	79.6	86.1	90.4	86.2
HIPTrack [3]	CVPR24	72.7	82.9	79.5	77.4	88.0	74.5	84.5	89.1	83.8
ODTrack-B [69]	AAAI24	73.2	83.2	80.6	77.0	87.9	75.1	85.1	90.1	84.9
F-BDMTrack-384 [63]	ICCV23	72.0	81.5	77.7	75.4	84.3	72.9	84.5	89.0	84.0
ROMTrack-384 [4]	ICCV23	71.4	81.4	78.2	74.2	84.3	72.4	84.1	89.0	83.7
ARTrack ₃₈₄ [56]	CVPR23	72.6	81.7	79.1	75.5	84.3	74.3	85.1	89.1	84.8
SeqTrack-B ₃₈₄ [6]	CVPR23	71.5	81.1	77.8	74.5	84.3	71.4	83.9	88.8	83.6
GRM [20]	CVPR23	69.9	79.3	75.8	73.4	82.9	70.4	84.0	88.7	83.3
OSTrack ₃₈₄ [64]	ECCV22	71.1	81.1	77.6	73.7	83.2	70.8	83.9	88.5	83.2
AiATrack [19]	ECCV22	69.0	79.4	73.8	69.6	80.0	63.2	82.7	87.8	80.4

TNL2K [54] comprises 700 test video sequences, each accompanied by natural language descriptions. As shown in Table 3, our method achieves state-of-the-art performance without utilizing natural language descriptions and surpasses existing vision-language trackers [21, 34].

UAV123 [42] is a dataset focusing on low-altitude drone aerial scenarios, consisting of 123 video sequences with an average length of 915 frames per sequence. Our method achieves state-of-the-art performance with comparable model sizes, demonstrating the capability of our approach in aerial scenes and small object tracking.

NfS [33] consists of 100 video sequences totaling 380,000 frames. Following previous works, we conduct evaluations on the 30 FPS version of the dataset. Our method rivals current state-of-the-art trackers in NfS. One possible reason for not achieving further improvement is that our method does not incorporate consecutive target position like ARTrack [56] and HIPTrack [3], which is crucial for NfS.

OTB2015 [59] is a classic dataset in visual tracking, consisting of 100 short-term tracking sequences that encompass 11 common challenges, such as target deformation, occlusion, and scale variation. Our method also achieves state-of-the-art performance on OTB2015.

4.3. Ablation Study

The Importance of Spatio-Temporal Context Modeling and TMoE. Table 5 demonstrates the significance of two core designs in our paper: spatio-temporal context modeling and TMoE. In Table 5, removing TMoE indicates direct fine-tuning with LoRA [25], while removing spatio-

Table 3. The performance of our method and other state-of-the-art trackers on TNL2K. The best three results are highlighted in **red**, **blue** and **bold**.

Method	AUC(%)	P_{Norm} (%)	P (%)
SPMTrack-G	64.7	82.6	70.6
SPMTrack-L	63.7	81.5	69.2
SPMTrack-B	62.0	79.7	66.7
LoRAT-B ₃₇₈ [37]	59.9	-	63.7
ODTrack-L [69]	61.7	-	-
ARTrackV2-L ₃₈₄ [2]	61.6	-	-
ARTrack-L ₃₈₄ [56]	60.3	-	-
RTracker-L [27]	60.6	-	63.7
UNINEXT-H [62]	59.3	-	62.8
CiteTracker [34]	57.7	-	59.6
VLT [21]	53.1	-	53.3

temporal modeling indicates using only the first frame template and search region as input and eliminating the target state token. Compared to LoRA, applying TMoE for parameter-efficient fine-tuning yields a substantial improvement of **+0.8** AUC on LaSOT, demonstrates the superiority of TMoE. And the spatio-temporal context modeling further enhances performance by an additional **+1.2** AUC. On the basis of incorporating spatio-temporal modeling, the improvement brought by TMoE is **+1.0** AUC, indicating that TMoE can help the model better capture spatio-temporal contextual information.

Where to Apply TMoE. Conventional MoE is typically applied to the FFN layers within Transformer blocks, while keeping the attention layers unchanged. In contrast, we ap-

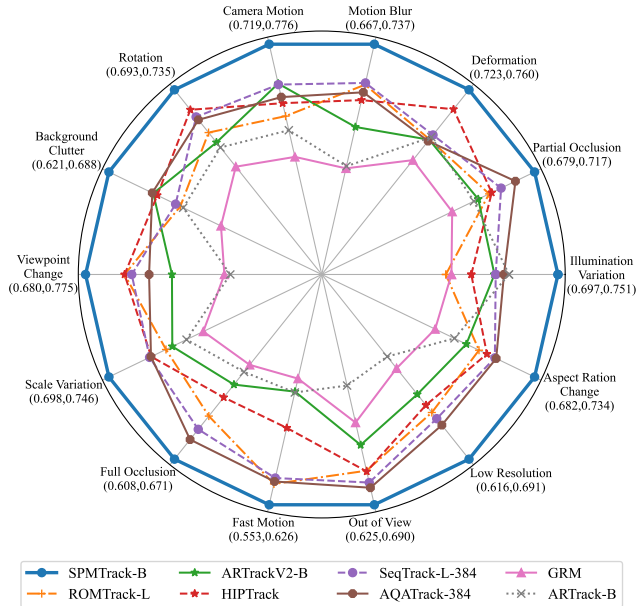


Figure 4. The performance of our method compared with other state-of-the-art trackers in terms of AUC across various scenarios in the LaSOT *test* split.

Table 4. The performance of our method and other state-of-the-art trackers on UAV123, NFS and OTB2015 in terms of AUC metrics. The best three results are highlighted in **red**, **blue** and **bold**.

Method	UAV123	NFS	OTB2015
SPMTrack-B	71.7	67.4	72.7
HIPTrack [3]	70.5	68.1	71.0
ARTrackV2-B [2]	69.9	67.6	-
ODTrack-L [69]	-	-	72.4
ARTrack ₃₈₄ [56]	70.5	66.8	-
SeqTrack-B ₃₈₄ [6]	68.6	66.7	-
DropTrack [57]	-	-	69.6
MixFormer-L [10]	69.5	-	-
STMTrack [16]	64.7	-	71.9

Table 5. Ablation studies on spatio-temporal context modeling and TMoE. Experiments are conducted on LaSOT.

#	Spatio-Temporal	TMoE	AUC (%)	P_{Norm} (%)	P (%)
1	✗	✗	72.9	81.9	79.1
2	✗	✓	73.7	82.7	80.0
3	✓	✗	73.9	82.8	80.0
4	✓	✓	74.9	84.0	81.7

ply TMoE in both the attention layers and the FFN layers. Table 6 demonstrates the impact of applying TMoE in different layers. Comparing the first, third, and fifth rows, applying TMoE to the query, key, value projections in attention layers and to FFN layers can both improve performance. Comparing the first, second and third rows, we find that applying TMoE in attention layers yields significantly

greater benefits compared to applying it only in FFN layers. Comparing the third and fourth rows, applying TMoE in the output projection matrix of the attention layer can bring a slight improvement.

Table 6. Ablation studies on applying TMoE in different layers. All results are evaluated on LaSOT *test* split. “✗” means replacing TMoE with LoRA.

#	QKV	Out Proj	FFN	AUC (%)	P_{Norm} (%)	P (%)
1	✗	✗	✗	73.9	82.8	80.0
2	✗	✗	✓	74.1	83.1	80.8
3	✓	✗	✗	74.5	83.6	81.2
4	✓	✓	✗	74.6	83.8	81.4
5	✓	✓	✓	74.9	84.0	81.7

Whether to use a shared compress expert. In TMoE, we employ a shared compression expert to reduce the input dimension to r , and use multiple routed experts for subsequent processing. As shown in the first and second rows of Table 7, compared to providing each routed expert with a compression expert, sharing the compression expert can achieve better performance while reducing the parameter count. When not sharing the compression expert, we provide t-SNE visualizations of the outputs from compression experts and routed experts in five TMoE modules in Figure 5. The outputs of different compression experts show significant overlaps, while the routed experts are more dispersed, validating the effectiveness of our approach.

TMoE vs. Conventional MoE. We compare TMoE with conventional MoE on the visual tracking task. For conventional MoE, we use LoRA to fine-tune the attention layers and apply MoE in the FFN layers with five experts: one frozen shared expert that copies pretrained FFN parameters, and four trainable routed experts, all routed experts are identical to the original FFN architecture, and a router is also applied. As shown in the first row and third row of Table 7, TMoE demonstrates significant advantages over conventional MoE in both parameter efficiency and performance.

Table 7. Ablation studies on whether to share the compression expert and use the conventional MoE to replace TMoE. Results are evaluated on LaSOT *test* split.

model variants	#Params(M)	AUC (%)	P_{Norm} (%)	P (%)
SPMTrack-B	115.3	74.9	84.0	81.7
w/o shared compress expert	131.3	74.8	83.7	81.5
Conventional MoE	316.8	73.4	82.6	79.8

The Number of Routed Experts. In Table 8, we evaluated the impact of different numbers of routed experts in TMoE. Results indicate that increasing the number of experts leads to improved performance, highlighting the potential of TMoE as a method to expand the parameter count and model scale. To balance the number of parameters and

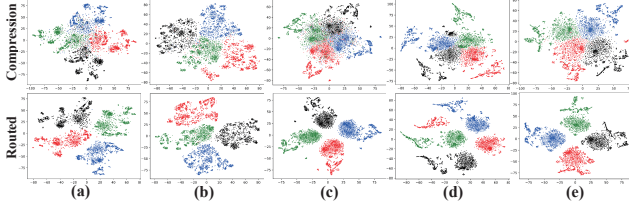


Figure 5. Comparison of t-SNE visualizations. Each column shows outputs from all compression experts (top) and routed experts (bottom) within a TMoE module. Different colors represent distinct experts. Zoom in for better view.



Figure 6. Visualization comparison of search region attention maps *with* and *without* TMoE. Zoom in for better view.

performance, we choose to use 4 experts, and whether there are separate optimal configurations for the TMoE in the attention layer and the FFN layer remains to be explored.

The Number of Reference Frames. In SPMTrack, we use the template and several tracked frames as reference frames to enhance the spatio-temporal modeling ability. In Table 9, we explore the impact of using different numbers of reference frames during training and inference. During inference, if only two reference frames are used, we simply select the frame at $\lfloor \frac{t}{2} \rfloor$ as the reference frame. If four reference frames are used, we select the frames at $\lfloor \frac{t}{4} \rfloor$, $\lfloor \frac{t}{2} \rfloor$, and $\lfloor \frac{3 \times t}{4} \rfloor$. As shown in Table 9, better performance can be achieved when the number of reference frames used during inference remains the same as that during training. Training with more reference frames can also lead to improved performance, illustrating that our method still has substantial potential for performance enhancement.

Comparison of attention maps with and without TMoE. In Figure 6, to exclude the influence of intermediate tracked frames, we use the model in rows 1 and 2 of Table 5 for comparison, where spatio-temporal modeling is removed

Table 8. The performance of our method on the *test* split of GOT-10K when setting different number of routed experts in TMoE.

Number	2	4	6	8
AO(%)	75.3	76.5	76.6	77.1
SR _{0.5} (%)	84.4	85.9	86.3	86.4
SR _{0.75} (%)	75.2	76.3	77.0	77.6

Table 9. Ablation study on the number of reference frames during training and inference. Results are evaluated based on SPMTrack-B on GOT-10K *test* split.

Training	Inference	AO (%)	SR _{0.5} (%)	SR _{0.75} (%)
2	2	75.8	85.1	75.3
	3	74.7	84.6	73.8
	4	69.8	81.8	66.2
3	2	73.1	83.9	72.7
	3	76.5	85.9	76.3
4	4	72.8	83.4	71.3
	2	70.6	83.9	68.9
	3	74.6	85.4	74.5
	4	77.5	87.3	77.2

and we focus solely on the impact of TMoE. We compare the attention maps of the search region in the last block of Transformer encoder. The first column is the template, the second column displays search region, the third column is the visualization result and pure attention map, as well as the fourth column. Figure 6 shows that when facing challenging scenarios such as occlusions, distractors, and viewpoint variations, TMoE effectively suppresses background regions while enhancing perception of the target boundary.

5. Conclusion

In this paper, we present TMoE, a mixture of experts module tailored for visual tracking, and propose SPMTrack, a novel tracker enabling spatio-temporal context modeling based on TMoE. TMoE is applied in the linear layers in both self-attention and FFN layers, enhancing the diversity and flexibility of expert combinations to better handle various relation modeling in visual tracking. Additionally, TMoE employs a lightweight and efficient structure and serves as a method of parameter-efficient fine-tuning, which enables us to train SPMTrack of larger scales and enables SPMTrack to achieve state-of-the-art performance with only a small subset of parameters need to be trained. Furthermore, we hope that this work will inspire more applications of mixture of experts in the field of visual tracking.

Acknowledgements. This paper was supported by Zhejiang Provincial Natural Science Foundation of China under Grant No.LD24F020016 and National Natural Science Foundation of China under Grant No.62176017.

SPMTrack: Spatio-Temporal Parameter-Efficient Fine-Tuning with Mixture of Experts for Scalable Visual Tracking

Supplementary Material

In the supplementary material, Section A presents additional ablation studies, further validating the effectiveness of other designs of SPMTrack and TMoE. In Section B, we provide more comprehensive performance comparisons between our SPMTrack and other excellent trackers. The comparisons consist of success curves on both overall LaSOT [14] *test* split and all challenging scenario subsets, along with overall precision curves. And in Section C, we further showcase the comparisons of tracking results of various trackers in complex scenarios and present more qualitative analyses of our method.

A. Further Analyses

A.1. Ablation Study on Target State Token

We employ a temporally propagated target state token to store historical target states, which is utilized in the prediction head for further adjustment and refinement of search region features. In Table A.1 and Table A.2, we remove the target state token and directly use the search region features from the output of feature extraction network for prediction in the prediction head. Table A.1 and Table A.2 present evaluation results on the GOT-10K [26] and TrackingNet [43] *test* splits, respectively. The results demonstrate that the integration of target state tokens, while introducing negligible additional parameters, improves performance on both two datasets, with a more significant improvement observed on TrackingNet.

Table A.1. Ablation study on whether adopt target state token. Results are evaluated on GOT-10K [26] *test* split.

model variants	#Params(M)	AO (%)	SR _{0.5} (%)	SR _{0.75} (%)
SPMTrack-B	115.331	76.5	85.9	76.3
w/o target state token	115.329	76.3	85.6	75.9

Table A.2. Ablation study on whether adopt target state token. Results are evaluated on TrackingNet [43] *test* split.

model variants	#Params(M)	AUC (%)	P_{Norm} (%)	P (%)
SPMTrack-B	115.331	86.1	90.2	85.6
w/o target state token	115.329	85.7	89.9	85.1

A.2. Ablation Study on Token Type Embedding

In SPMTrack, we add not only positional embedding but also token type embeddings to the input of the feature ex-

traction network to further enhance the token information. The additional parameter count and computational overhead introduced by the token type embeddings are negligible.

In Table A.3, we investigate the impact of introducing different token type embeddings on the performance of SPMTrack-B. Comparing the first row and the third row in Table A.3, adding three types of token type embeddings leads to a performance improvement. Comparing the first row and second row, we find that when the type embedding corresponding to the target foreground tokens is not introduced, which means all tokens in the reference frames use the same type embedding, there are no performance gains observed. The results indicate that the target foreground token type embedding is the most crucial among the three categories, as it enhances the ability of the tracker to discriminate target foreground regions, thereby improving performance.

Table A.3. Ablation study on different token type embeddings, where TE_o , TE_b and TE_S represent the type embeddings of the foreground region tokens, background region tokens in reference frames and the search region tokens, respectively.

#	TE_o	TE_b	TE_S	AO (%)	SR _{0.5} (%)	SR _{0.75} (%)
1	x	x	x	76.2	85.6	75.8
2	x	✓	✓	76.2	85.5	76.0
3	✓	✓	✓	76.5	85.9	76.3

A.3. Ablation Study on Different Pre-trained Models

In this paper, we select DINOv2 [44] as the pre-trained model. In Table A.4, we investigate the impact of different pre-trained models on the final performance. All experiments are conducted based on SPMTrack-B, with pre-trained models based on the ViT-B [12] architecture. It is worth noting that for pre-trained models with an image patch size of 16, we use a reference frame size of 192×192 and a search region size of 384×384 . As shown in Table A.4, experimental results demonstrate that SPMTrack maintains consistent performance on GOT-10K regardless of the choice of pre-trained model, indicating the robustness and the generalization ability of our approach. Eventually, in order to make a fair comparison with LoRAT [37] that also employs parameter-efficient fine-tuning, we still select DINOv2 [44] as the pre-trained model.

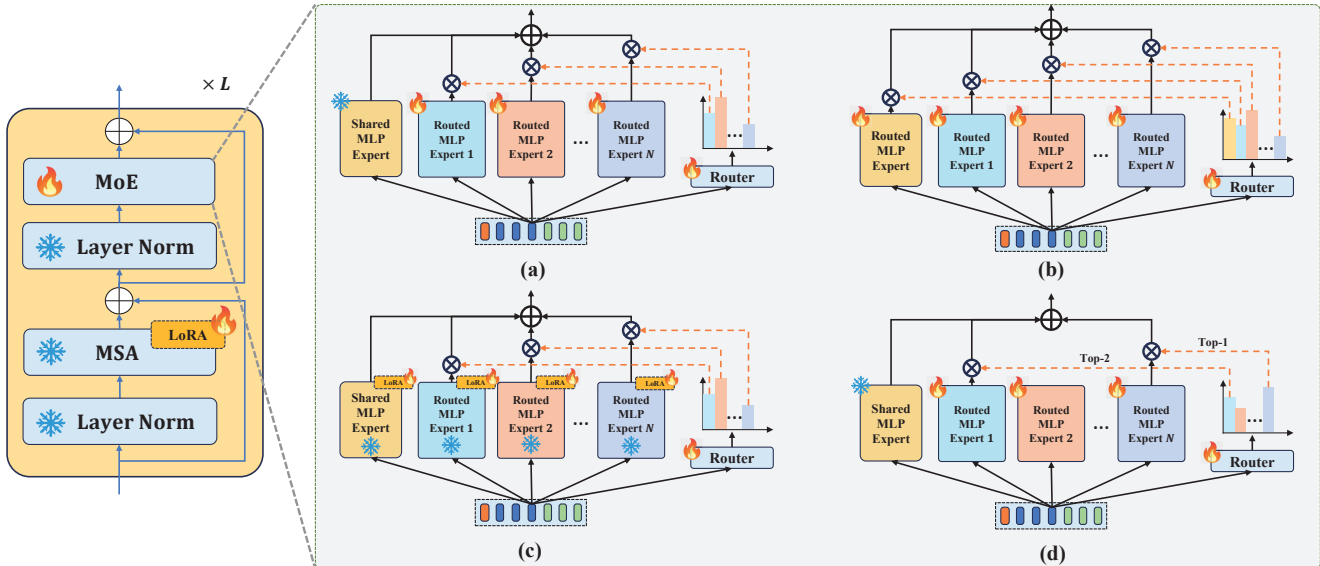


Figure A.1. Several conventional MoE architectural designs, where MoE modules exclusively replace feed-forward network (FFN) layers in the original Transformer Block, while linear layers in multi-head self-attention are fine-tuned using LoRA [25]. Zoom in for better view.

Table A.4. Ablation study on different pre-trained models. Results are evaluated on GOT-10K *test* split.

Pretrained Models	Patch Size	AO (%)	SR _{0.5} (%)	SR _{0.75} (%)
DINOv2 [44]	14	76.5	85.9	76.3
MAE [22]	16	76.3	87.0	75.1
DropMAE [57]	16	76.6	87.7	74.0

A.4. Ablation Study on MLP Prediction Head

In SPMTrack, in order to make a fair comparison with LoRAT [37], we also adopt a fully MLP-based prediction head. However, this does not represent our optimal configuration. As demonstrated in Table A.5, we replace the MLP prediction head with the convolution-based prediction head used in previous trackers like OSTRack [64]. Although the MLP prediction head has fewer parameters, the overall model parameter difference is minimal, and the convolution-based head achieves significantly superior performance. In contrast to LoRAT, which fails completely under parameter-efficient fine-tuning when using convolution-based heads, our method achieves even better performance with convolution-based heads, which further demonstrates the generality of our proposed TMoE for parameter-efficient fine-tuning and also further demonstrates the potential for performance improvement in SPMTrack.

A.5. More Comparisons with Conventional MoE

In Table 7 of the main manuscript, we compare our method with conventional MoE in terms of parameter count and per-

Table A.5. Ablation study on MLP-based prediction head and convolutional-based prediction head. Results are evaluated on GOT-10K *test* split.

Prediction Head	#Params(M)	AO (%)	SR _{0.5} (%)	SR _{0.75} (%)
MLP Head	2.37	76.5	85.9	76.3
OSTrack [64] Conv Head	6.47	76.8	86.4	77.0

formance on LaSOT, the conventional MoE structure in Table 7 is illustrated in Figure A.1(a), most current large language models adopt a similar architecture [9, 11, 15, 40, 46, 58]. Additionally, as shown in Figure A.1, we explore various alternative MoE structures. Figure A.1(b) shows a modification of the architecture in Figure A.1(a) where we replace the frozen shared expert with a learnable routed expert and initialize all five routed experts with corresponding FFN weights from the pre-trained model. Figure A.1(c) extends the design in Figure A.1(a) by freezing all experts and fine-tuning each expert using LoRA [25]. In Figure A.1(d), we adopt the way of sparsely activating experts with top-k routing scores on the basis of Figure A.1(a). The experimental results of these different MoE architectures on LaSOT *test* split are presented in Table A.6.

As shown in Table A.6, in row 1, the MoE comprises one shared expert and four routed experts, with all experts participating in computation, hence the expert count is 1+4 as well as the activated expert count. Row 3 follows the same rule. In row 2, there are only five routed experts, and all of them participate in the computation. In row 4, the MoE includes a total of one shared expert and four routed experts, but only the routed experts with the top-2 routing

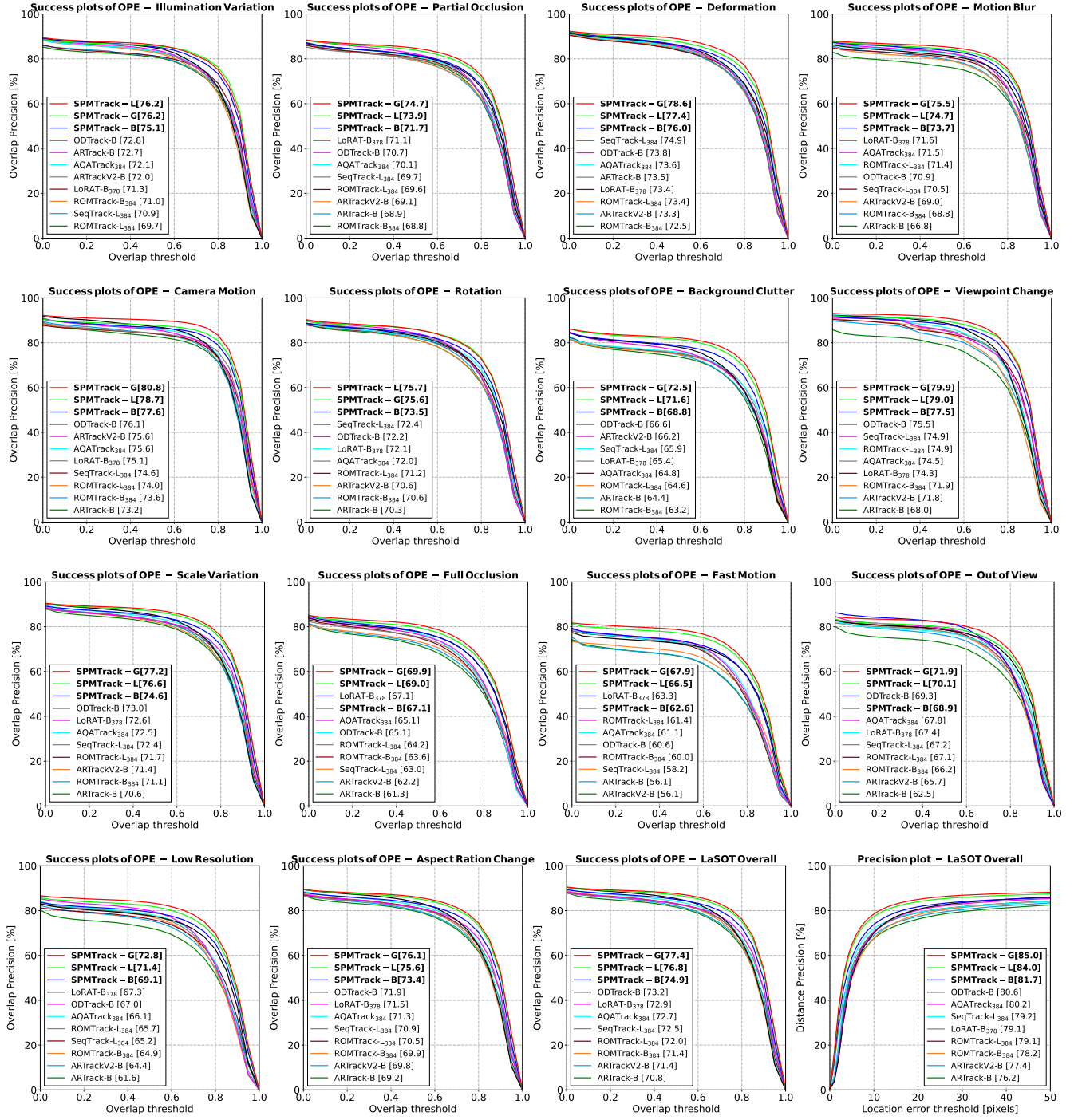
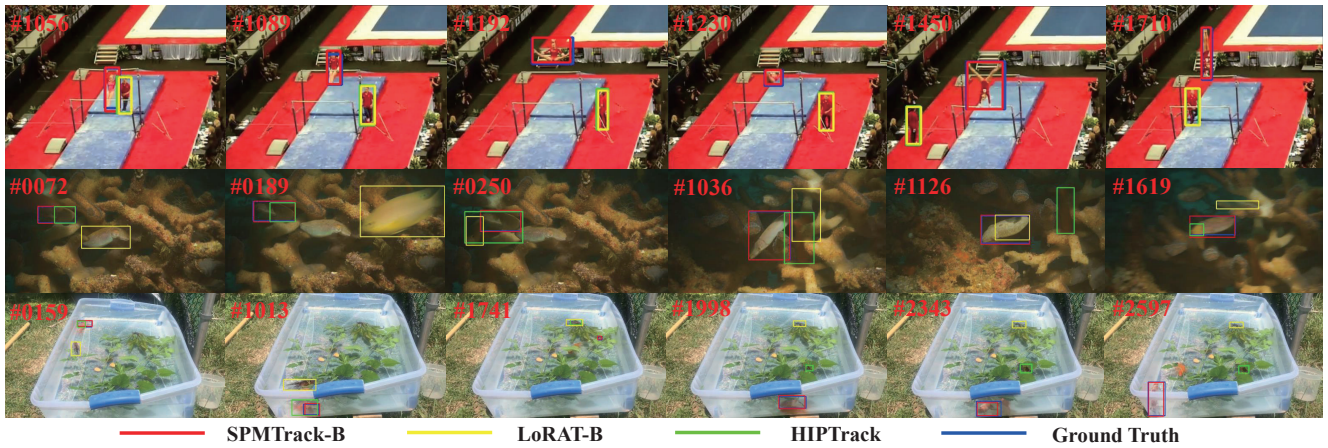


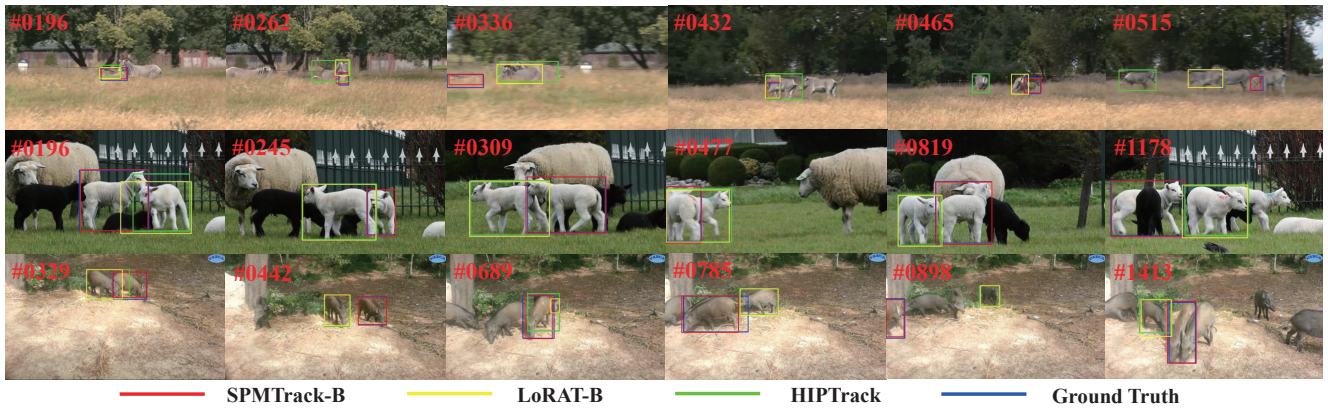
Figure A.2. Comparisons of our proposed SPMTrack with other excellent trackers in the success curve on LaSOT *test* split, which includes eleven challenging scenarios such as Low Resolution, Motion Blur, Scale Variation, etc. We also provide the comparisons of the success and precision curves across the entire LaSOT *test* split. Zoom in for better view.

scores are activated, so the number of activated experts is 1 + 2. In row 5, the MoE includes a total of one shared experts and eight routed experts, and the routed experts with the top-4 routing scores are activated.

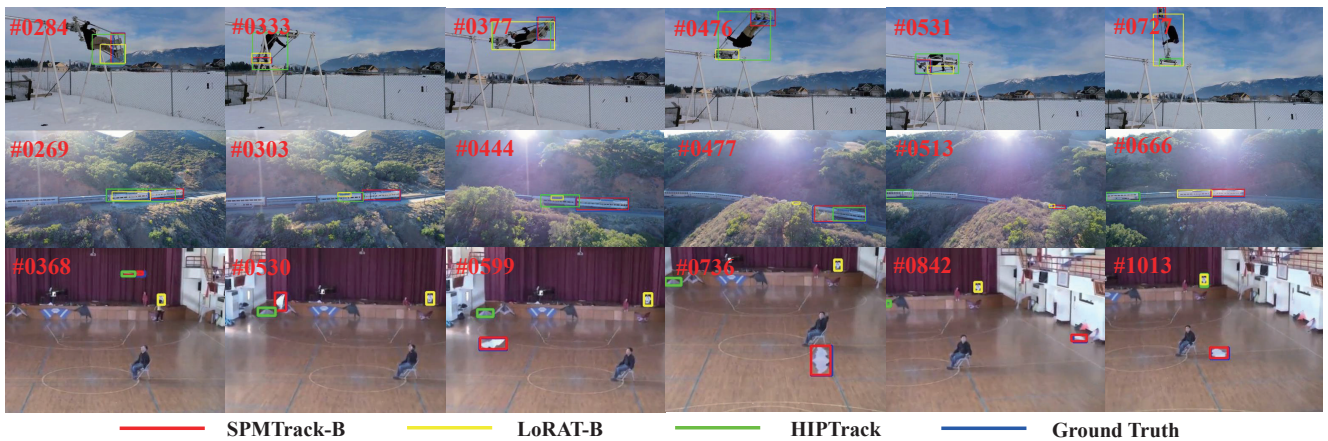
Table A.6 demonstrates that TMoE achieves superior performance compared to all conventional MoE approaches that are only applied to replace FFN layers, while maintaining significantly lower total parameters (all conventional



(a) Qualitative results of three methods when the targets undergo large deformations.



(b) Qualitative results of three methods when the targets suffer from partial occlusions.



(c) Qualitative results of three methods when the targets have large scale variations.

Figure A.3. This figure presents a visual comparison among our proposed SPMTrack-B, LoRAT-B [37] and HIPTrack [3] in the challenges of target deformation, partial occlusion and scale variation. It demonstrates that our method achieves more effective and accurate tracking in the aforementioned challenging scenarios. Zoom in for better view.

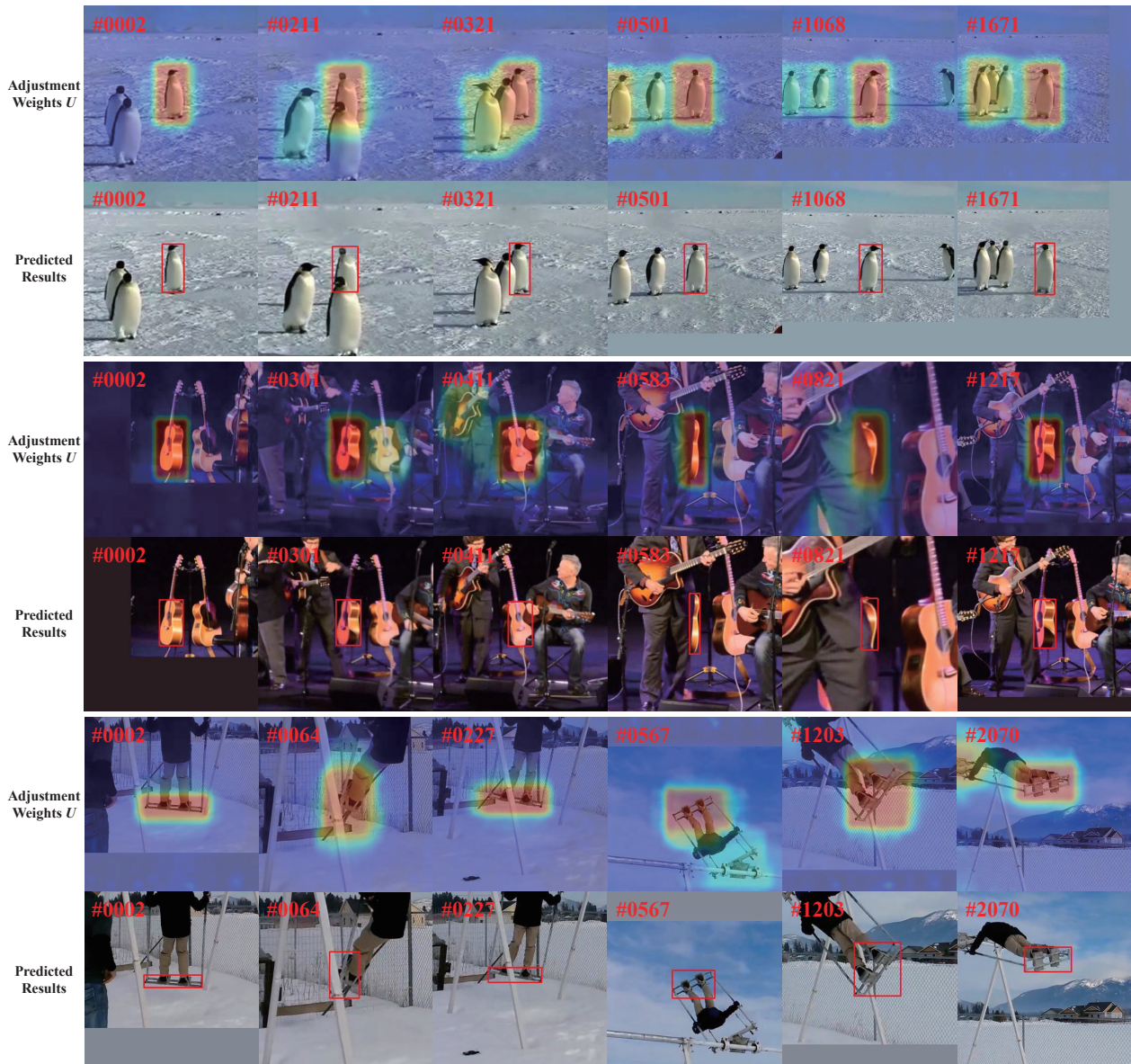


Figure A.4. Visualization of the search region feature adjustment weights U and the corresponding predicted bounding boxes.

MoE variants exceed 300M parameters). At the same time, comparing row 2 with other rows, we observe that preserve pre-trained weights in MoE leads to substantially improved performance. This explains why row 3 achieves optimal performance among all conventional MoE approaches. Comparing rows 1, 4, and 5, we find that increasing the overall parameter count or the number of activated experts results in only marginal performance gains, further validating the effectiveness of our TMoE design.

The experimental results indicate that when using conventional MoE, the performance on visual tracking is inferior to that of TMoE. However, this does not mean that

TMoE can achieve better performance on large language models. For example, the reinforcement learning [28–30, 41, 66–68] phase of LLM requires routing replay to ensure stability, and our finer-grained expert design also leads to an increase in the number of routing operations, which raises the difficulty of training.

At the same time, in the field of natural language processing, sparsely activated MoE is the mainstream. But sparsely activated MoE requires more engineering optimizations. Due to the limitations of time and resources, we have not further explored the performance of TMoE under sparse activation. We also hope that this work can inspire

other researchers to conduct related explorations in the field of visual tracking.

Table A.6. Performance comparison between different conventional MoE approaches and TMoE. The number of experts is represented in the form of $a + b$, where a represents shared experts and b represents routed experts. All results are evaluated on LaSOT *test* split.

MoE Variants	#MLP Experts	#Activated Experts	AUC (%)	P_{Norm} (%)	P (%)
Figure A.1(a)	1+4	1+4	73.4	82.6	79.8
Figure A.1(b)	5	5	72.7	81.5	78.7
Figure A.1(c)	1+4	1+4	74.4	83.4	80.6
Figure A.1(d)	1+4	1+2	73.3	82.0	79.4
	1+8	1+4	73.8	82.8	79.9
TMoE	-	-	74.9	84.0	81.7

B. More Detailed Results in Different Attribute Scenes on LaSOT

In Figure A.2, we provide a more detailed comparison of our method with other current state-of-the-art trackers LoRAT [37], ODTrack [69], ARTrackV2 [2], AQATrack [61], ARTrack [56], ROMTrack [4] and SeqTrack [6] across various challenging scenario subsets in LaSOT [14]. Figure A.2 presents detailed success curves and AUC scores across individual subsets, along with the success and precision curves on the entire LaSOT *test* split. The results demonstrate that SPMTrack-B significantly outperforms current state-of-the-art approaches both overall and across the vast majority of subsets.

C. More Qualitative Results

C.1. Tracking Results

In order to visually highlight the advantages of our method over existing approaches in challenging scenarios, we provide additional visualization results in Figure A.3. All videos are from the *test* split of LaSOT. We compare our proposed SPMTrack-B with HIPTrack [3] and LoRAT-B [37] in terms of performance when the target undergoes deformation, occlusion, and scale variation. All the selected videos are challenging, as described below:

- Figure A.3(a) demonstrates the tracking results of three methods when the target suffers deformations.
- Figure A.3(b) demonstrates the tracking results of three methods when the target suffers partial occlusions.
- Figure A.3(c) demonstrates the tracking results of three methods when the target suffers scale variations.

C.2. Visualization of Search Region Feature Adjustment Weight

In the prediction head of SPMTrack, we compute matrix multiplication between the output H' corresponding to target state token and the output search region feature X' to obtain weight U . The obtained weight U contains the historical state information of the target and is used to further adjust and refine the output search region feature X' . In Figure A.4, we visualize the weight U . The visualization results demonstrate that the adjustment weight U can significantly distinguish between the target foreground region and irrelevant background regions. Moreover, the heatmaps exhibit patterns resembling bounding boxes, with substantially higher weights inside the “bounding box”. This further enhances the features at potential target locations, thereby improving the foreground-background discrimination capability of the search region features.

References

- [1] Rahaf Aljundi, Punarjay Chakravarty, and Tinne Tuytelaars. Expert gate: Lifelong learning with a network of experts. In *Proceedings of the IEEE Conference on Computer Vision and Pattern Recognition (CVPR)*, 2017. 2
- [2] Yifan Bai, Zeyang Zhao, Yihong Gong, and Xing Wei. Ar-trackv2: Prompting autoregressive tracker where to look and how to describe. In *Proceedings of the IEEE/CVF Conference on Computer Vision and Pattern Recognition (CVPR)*, pages 19048–19057, 2024. 2, 5, 6, 7, 14
- [3] Wenrui Cai, Qingjie Liu, and Yunhong Wang. Hiptrack: Visual tracking with historical prompts. In *Proceedings of the IEEE/CVF Conference on Computer Vision and Pattern Recognition (CVPR)*, pages 19258–19267, 2024. 1, 2, 3, 5, 6, 7, 12, 14
- [4] Yidong Cai, Jie Liu, Jie Tang, and Gangshan Wu. Robust object modeling for visual tracking. In *Proceedings of the IEEE/CVF International Conference on Computer Vision (ICCV)*, pages 9589–9600, 2023. 1, 2, 5, 6, 14
- [5] Boyu Chen, Peixia Li, Lei Bai, Lei Qiao, Qihong Shen, Bo Li, Weihao Gan, Wei Wu, and Wanli Ouyang. Backbone is all your need: a simplified architecture for visual object tracking. In *Computer Vision—ECCV 2022: 17th European Conference, Tel Aviv, Israel, October 23–27, 2022, Proceedings, Part XXII*, pages 375–392. Springer, 2022. 1, 2
- [6] Xin Chen, Houwen Peng, Dong Wang, Huchuan Lu, and Han Hu. Seqtrack: Sequence to sequence learning for visual object tracking. In *Proceedings of the IEEE/CVF Conference on Computer Vision and Pattern Recognition (CVPR)*, pages 14572–14581, 2023. 2, 5, 6, 7, 14
- [7] Yucheng Chen and Lin Wang. emoe-tracker: Environmental moe-based transformer for robust event-guided object tracking. *arXiv preprint arXiv:2406.20024*, 2024. 2
- [8] Mohammed Nowaz Rabbani Chowdhury, Shuai Zhang, Meng Wang, Sijia Liu, and Pin-Yu Chen. Patch-level routing in mixture-of-experts is provably sample-efficient for convolutional neural networks. In *Proceedings of the 40th Interna-*

- tional Conference on Machine Learning*, pages 6074–6114. PMLR, 2023. [2](#)
- [9] Aidan Clark, Diego de Las Casas, Aurelia Guy, Arthur Mensch, Michela Paganini, Jordan Hoffmann, Bogdan Damoc, Blake Hechtman, Trevor Cai, Sebastian Borgeaud, et al. Unified scaling laws for routed language models. In *International conference on machine learning*, pages 4057–4086. PMLR, 2022. [2](#), [10](#)
- [10] Yutao Cui, Cheng Jiang, Limin Wang, and Gangshan Wu. Mixformer: End-to-end tracking with iterative mixed attention. In *Proceedings of the IEEE/CVF Conference on Computer Vision and Pattern Recognition (CVPR)*, pages 13608–13618, 2022. [1](#), [2](#), [7](#)
- [11] Damai Dai, Chengqi Deng, Chenggang Zhao, R.x. Xu, Huazuo Gao, Deli Chen, Jiashi Li, Wangding Zeng, Xingkai Yu, Y. Wu, Zhenda Xie, Y.k. Li, Panpan Huang, Fuli Luo, Chong Ruan, Zhifang Sui, and Wenfeng Liang. DeepSeek-MoE: Towards ultimate expert specialization in mixture-of-experts language models. In *Proceedings of the 62nd Annual Meeting of the Association for Computational Linguistics (Volume 1: Long Papers)*, pages 1280–1297, Bangkok, Thailand, 2024. Association for Computational Linguistics. [2](#), [10](#)
- [12] Alexey Dosovitskiy, Lucas Beyer, Alexander Kolesnikov, Dirk Weissenborn, Xiaohua Zhai, Thomas Unterthiner, Mostafa Dehghani, Matthias Minderer, Georg Heigold, Sylvain Gelly, et al. An image is worth 16x16 words: Transformers for image recognition at scale. In *ICLR*, 2021. [1](#), [2](#), [3](#), [5](#), [9](#)
- [13] Nan Du, Yanping Huang, Andrew M Dai, Simon Tong, Dmitry Lepikhin, Yuanzhong Xu, Maxim Krikun, Yanqi Zhou, Adams Wei Yu, Orhan Firat, Barret Zoph, Liam Fedus, Maarten P Bosma, Zongwei Zhou, Tao Wang, Emma Wang, Kellie Webster, Marie Pellat, Kevin Robinson, Kathleen Meier-Hellstern, Toju Duke, Lucas Dixon, Kun Zhang, Quoc Le, Yonghui Wu, Zhifeng Chen, and Claire Cui. GLaM: Efficient scaling of language models with mixture-of-experts. In *Proceedings of the 39th International Conference on Machine Learning*, pages 5547–5569. PMLR, 2022. [2](#)
- [14] Heng Fan, Liting Lin, Fan Yang, Peng Chu, Ge Deng, Sijia Yu, Hexin Bai, Yong Xu, Chunyuan Liao, and Haibin Ling. Lasot: A high-quality benchmark for large-scale single object tracking. In *CVPR*, pages 5374–5383, 2019. [2](#), [5](#), [9](#), [14](#)
- [15] William Fedus, Barret Zoph, and Noam Shazeer. Switch transformers: Scaling to trillion parameter models with simple and efficient sparsity. *Journal of Machine Learning Research*, 23(120):1–39, 2022. [2](#), [10](#)
- [16] Zhihong Fu, Qingjie Liu, Zehua Fu, and Yunhong Wang. Stmtrack: Template-free visual tracking with space-time memory networks. In *CVPR*, pages 13774–13783, 2021. [7](#)
- [17] Zhihong Fu, Zehua Fu, Qingjie Liu, Wenrui Cai, and Yunhong Wang. Sparset: Visual tracking with sparse transformers. In *Proceedings of the Thirtieth International Joint Conference on Artificial Intelligence, IJCAI-22*, pages 905–912, 2022. [1](#)
- [18] Peng Gao, Shijie Geng, Renrui Zhang, Teli Ma, Rongyao Fang, Yongfeng Zhang, Hongsheng Li, and Yu Qiao. Clip-adapter: Better vision-language models with feature adapters. *International Journal of Computer Vision*, 132(2): 581–595, 2024. [3](#)
- [19] Shenyuan Gao, Chunlun Zhou, Chao Ma, Xinggang Wang, and Junsong Yuan. Aiatrack: Attention in attention for transformer visual tracking. In *Computer Vision–ECCV 2022: 17th European Conference, Tel Aviv, Israel, October 23–27, 2022, Proceedings, Part XXII*, pages 146–164. Springer, 2022. [1](#), [6](#)
- [20] Shenyuan Gao, Chunlun Zhou, and Jun Zhang. Generalized relation modeling for transformer tracking. In *Proceedings of the IEEE/CVF Conference on Computer Vision and Pattern Recognition (CVPR)*, pages 18686–18695, 2023. [1](#), [2](#), [5](#), [6](#)
- [21] Mingzhe Guo, Zhipeng Zhang, Heng Fan, and Liping Jing. Divert more attention to vision-language tracking. In *Advances in Neural Information Processing Systems*, pages 4446–4460. Curran Associates, Inc., 2022. [6](#)
- [22] Kaiming He, Xinlei Chen, Saining Xie, Yanghao Li, Piotr Dollár, and Ross Girshick. Masked autoencoders are scalable vision learners. In *Proceedings of the IEEE/CVF Conference on Computer Vision and Pattern Recognition (CVPR)*, pages 16000–16009, 2022. [10](#)
- [23] Kaijie He, Canlong Zhang, Sheng Xie, Zhixin Li, and Zhiwen Wang. Target-aware tracking with long-term context attention. *Proceedings of the AAAI Conference on Artificial Intelligence*, 37(1):773–780, 2023. [2](#)
- [24] Neil Houlsby, Andrei Giurgiu, Stanislaw Jastrzebski, Bruna Morrone, Quentin De Laroussilhe, Andrea Gesmundo, Mona Attariyan, and Sylvain Gelly. Parameter-efficient transfer learning for nlp. In *International conference on machine learning*, pages 2790–2799. PMLR, 2019. [2](#), [3](#)
- [25] Edward J. Hu, Yelong Shen, Phillip Wallis, Zeyuan Allen-Zhu, Yuanzhi Li, Shean Wang, Lu Wang, and Weizhu Chen. Lora: Low-rank adaptation of large language models. In *The Tenth International Conference on Learning Representations, ICLR*, 2022. [3](#), [6](#), [10](#)
- [26] Lianghua Huang, Xin Zhao, and Kaiqi Huang. Got-10k: A large high-diversity benchmark for generic object tracking in the wild. *TPAMI*, 2019. [2](#), [5](#), [9](#)
- [27] Yuqing Huang, Xin Li, Zikun Zhou, Yaowei Wang, Zhenyu He, and Ming-Hsuan Yang. Rtracker: Recoverable tracking via pn tree structured memory. In *Proceedings of the IEEE/CVF Conference on Computer Vision and Pattern Recognition (CVPR)*, pages 19038–19047, 2024. [6](#)
- [28] Zixuan Huang, Yikun Ban, Lean Fu, Xiaojie Li, Zhongxiang Dai, Jianxin Li, and Deqing Wang. Adaptive batch-wise sample scheduling for direct preference optimization, 2026. [13](#)
- [29] Zixuan Huang, Xin Xia, Yuxi Ren, Jianbin Zheng, Xuanda Wang, Zhixia Zhang, Hongyan Xie, Songshi Liang, Zehao Chen, Xuefeng Xiao, Fuzhen Zhuang, Jianxin Li, Yikun Ban, and Deqing Wang. Does your reasoning model implicitly know when to stop thinking?, 2026.
- [30] Zixuan Huang, Xin Xia, Yuxi Ren, Jianbin Zheng, Xuefeng Xiao, Hongyan Xie, Li Huaqiu, Songshi Liang, Zhongxiang

- Dai, Fuzhen Zhuang, Jianxin Li, Yikun Ban, and Deqing Wang. Real-time aligned reward model beyond semantics, 2026. 13
- [31] Robert A Jacobs, Michael I Jordan, Steven J Nowlan, and Geoffrey E Hinton. Adaptive mixtures of local experts. *Neural computation*, 3(1):79–87, 1991. 2
- [32] Menglin Jia, Luming Tang, Bor-Chun Chen, Claire Cardie, Serge Belongie, Bharath Hariharan, and Ser-Nam Lim. Visual prompt tuning. In *European Conference on Computer Vision*, pages 709–727. Springer, 2022. 3
- [33] Hamed Kiani Galoogahi, Ashton Fagg, Chen Huang, Deva Ramanan, and Simon Lucey. Need for speed: A benchmark for higher frame rate object tracking. In *Proceedings of the IEEE International Conference on Computer Vision (ICCV)*, 2017. 6
- [34] Xin Li, Yuqing Huang, Zhenyu He, Yaowei Wang, Huchuan Lu, and Ming-Hsuan Yang. Citetracker: Correlating image and text for visual tracking. In *Proceedings of the IEEE/CVF International Conference on Computer Vision (ICCV)*, pages 9974–9983, 2023. 6
- [35] Xiang Lisa Li and Percy Liang. Prefix-tuning: Optimizing continuous prompts for generation. In *Proceedings of the 59th Annual Meeting of the Association for Computational Linguistics and the 11th International Joint Conference on Natural Language Processing (Volume 1: Long Papers)*, pages 4582–4597, 2021. 3
- [36] Liting Lin, Heng Fan, Zhipeng Zhang, Yong Xu, and Haibin Ling. Swintrack: A simple and strong baseline for transformer tracking. *Advances in Neural Information Processing Systems*, 35:16743–16754, 2022. 3
- [37] Liting Lin, Heng Fan, Zhipeng Zhang, Yaowei Wang, Yong Xu, and Haibin Ling. Tracking meets lora: Faster training, larger model, stronger performance. In *Computer Vision – ECCV 2024*, pages 300–318, Cham, 2025. Springer Nature Switzerland. 1, 3, 4, 5, 6, 9, 10, 12, 14
- [38] Tsung-Yi Lin, Michael Maire, Serge Belongie, James Hays, Pietro Perona, Deva Ramanan, Piotr Dollár, and C Lawrence Zitnick. Microsoft coco: Common objects in context. In *ECCV*, pages 740–755, 2014. 5
- [39] Ilya Loshchilov and Frank Hutter. Decoupled weight decay regularization. In *7th International Conference on Learning Representations, ICLR*, 2019. 5
- [40] Jiaqi Ma, Zhe Zhao, Xinyang Yi, Jilin Chen, Lichan Hong, and Ed H Chi. Modeling task relationships in multi-task learning with multi-gate mixture-of-experts. In *Proceedings of the 24th ACM SIGKDD international conference on knowledge discovery & data mining*, pages 1930–1939, 2018. 2, 10
- [41] Wenhan Ma, Hailin Zhang, Liang Zhao, Yifan Song, Yudong Wang, Zhifang Sui, and Fuli Luo. Stabilizing moe reinforcement learning by aligning training and inference routers, 2025. 13
- [42] Matthias Mueller, Neil Smith, and Bernard Ghanem. A benchmark and simulator for uav tracking. In *ECCV*, pages 445–461, 2016. 6
- [43] Matthias Muller, Adel Bibi, Silvio Giancola, Salman Alsubaihi, and Bernard Ghanem. Trackingnet: A large-scale dataset and benchmark for object tracking in the wild. In *ECCV*, pages 300–317, 2018. 2, 5, 9
- [44] Maxime Oquab, Timothée Darcet, Théo Moutakanni, Huy Vo, Marc Szafraniec, Vasil Khalidov, Pierre Fernandez, Daniel Haziza, Francisco Massa, Alaaeldin El-Nouby, et al. Dinov2: Learning robust visual features without supervision. *Transactions on Machine Learning Research Journal*, pages 1–31, 2024. 5, 9, 10
- [45] Jonas Pfeiffer, Andreas Rücklé, Clifton Poth, Aishwarya Kamath, Ivan Vulić, Sebastian Ruder, Kyunghyun Cho, and Iryna Gurevych. Adapterhub: A framework for adapting transformers. In *Proceedings of the 2020 Conference on Empirical Methods in Natural Language Processing: System Demonstrations*, pages 46–54, 2020. 3
- [46] Joan Puigcerver, Carlos Riquelme Ruiz, Basil Mustafa, and Neil Houlsby. From sparse to soft mixtures of experts. In *The Twelfth International Conference on Learning Representations, ICLR*, 2024. 2, 10
- [47] Hamid Rezaatoughi, Nathan Tsoi, JunYoung Gwak, Amir Sadeghian, Ian Reid, and Silvio Savarese. Generalized intersection over union: A metric and a loss for bounding box regression. In *CVPR*, pages 658–666, 2019. 5
- [48] Carlos Riquelme, Joan Puigcerver, Basil Mustafa, Maxim Neumann, Rodolphe Jenatton, André Susano Pinto, Daniel Keysers, and Neil Houlsby. Scaling vision with sparse mixture of experts. In *Advances in Neural Information Processing Systems*, pages 8583–8595. Curran Associates, Inc., 2021. 2
- [49] Zhangyong Tang, Tianyang Xu, Zhenhua Feng, Xuefeng Zhu, He Wang, Pengcheng Shao, Chunyang Cheng, Xiaojun Wu, Muhammad Awais, Sara Atito, et al. Revisiting rgbt tracking benchmarks from the perspective of modality validity: A new benchmark, problem, and method. *arXiv preprint arXiv:2405.00168*, 2024. 2
- [50] Chunlin Tian, Zhan Shi, Zhijiang Guo, Li Li, and Chengzhong Xu. Hydralora: An asymmetric lora architecture for efficient fine-tuning. In *Advances in Neural Information Processing Systems (NeurIPS)*, 2024. 3, 4
- [51] Ashish Vaswani, Noam Shazeer, Niki Parmar, Jakob Uszkoreit, Llion Jones, Aidan N Gomez, Łukasz Kaiser, and Illia Polosukhin. Attention is all you need. In *NIPS*, pages 5998–6008, 2017. 1
- [52] Guangting Wang, Chong Luo, Xiaoyan Sun, Zhiwei Xiong, and Wenjun Zeng. Tracking by instance detection: A meta-learning approach. In *CVPR*, pages 6288–6297, 2020. 5
- [53] Ke Wang, Jiahui Zhu, Minjie Ren, Zeming Liu, Shiwei Li, Zongye Zhang, Chenkai Zhang, Xiaoyu Wu, Qiqi Zhan, Qingjie Liu, et al. A survey on data synthesis and augmentation for large language models. *arXiv preprint arXiv:2410.12896*, 2024. 2
- [54] Xiao Wang, Xiujun Shu, Zhipeng Zhang, Bo Jiang, Yaowei Wang, Yonghong Tian, and Feng Wu. Towards more flexible and accurate object tracking with natural language: Algorithms and benchmark. In *Proceedings of the IEEE/CVF Conference on Computer Vision and Pattern Recognition (CVPR)*, pages 13763–13773, 2021. 2, 6
- [55] Zifeng Wang, Zizhao Zhang, Chen-Yu Lee, Han Zhang, Ruoxi Sun, Xiaoqi Ren, Guolong Su, Vincent Perot, Jennifer

- Dy, and Tomas Pfister. Learning to prompt for continual learning. In *Proceedings of the IEEE/CVF Conference on Computer Vision and Pattern Recognition*, pages 139–149, 2022. 3
- [56] Xing Wei, Yifan Bai, Yongchao Zheng, Dahu Shi, and Yihong Gong. Autoregressive visual tracking. In *Proceedings of the IEEE/CVF Conference on Computer Vision and Pattern Recognition (CVPR)*, pages 9697–9706, 2023. 2, 5, 6, 7, 14
- [57] Qiangqiang Wu, Tianyu Yang, Ziquan Liu, Baoyuan Wu, Ying Shan, and Antoni B. Chan. Dropmae: Masked autoencoders with spatial-attention dropout for tracking tasks. In *Proceedings of the IEEE/CVF Conference on Computer Vision and Pattern Recognition (CVPR)*, pages 14561–14571, 2023. 1, 7, 10
- [58] Xun Wu, Shaohan Huang, and Furu Wei. Mixture of lora experts. In *The Twelfth International Conference on Learning Representations, ICLR*, 2024. 2, 10
- [59] Y. Wu, J. Lim, and M. Yang. Object tracking benchmark. *TPAMI*, 37(9):1834–1848, 2015. 6
- [60] Fei Xie, Chunyu Wang, Guangting Wang, Yue Cao, Wankou Yang, and Wenjun Zeng. Correlation-aware deep tracking. In *Proceedings of the IEEE/CVF Conference on Computer Vision and Pattern Recognition (CVPR)*, pages 8751–8760, 2022. 2
- [61] Jinxia Xie, Bineng Zhong, Zhiyi Mo, Shengping Zhang, Liangtao Shi, Shuxiang Song, and Rongrong Ji. Autoregressive queries for adaptive tracking with spatio-temporal transformers. In *Proceedings of the IEEE/CVF Conference on Computer Vision and Pattern Recognition (CVPR)*, pages 19300–19309, 2024. 5, 6, 14
- [62] Bin Yan, Yi Jiang, Jiannan Wu, Dong Wang, Ping Luo, Zehuan Yuan, and Huchuan Lu. Universal instance perception as object discovery and retrieval. In *Proceedings of the IEEE/CVF Conference on Computer Vision and Pattern Recognition (CVPR)*, pages 15325–15336, 2023. 6
- [63] Dawei Yang, Jianfeng He, Yinchao Ma, Qianjin Yu, and Tianzhu Zhang. Foreground-background distribution modeling transformer for visual object tracking. In *Proceedings of the IEEE/CVF International Conference on Computer Vision (ICCV)*, pages 10117–10127, 2023. 1, 2, 6
- [64] Botao Ye, Hong Chang, Bingpeng Ma, Shiguang Shan, and Xilin Chen. Joint feature learning and relation modeling for tracking: A one-stream framework. In *European Conference on Computer Vision*, pages 341–357. Springer, 2022. 1, 2, 5, 6, 10
- [65] Yihua Zhang, Ruisi Cai, Tianlong Chen, Guanhua Zhang, Huan Zhang, Pin-Yu Chen, Shiyu Chang, Zhangyang Wang, and Sijia Liu. Robust mixture-of-expert training for convolutional neural networks. In *Proceedings of the IEEE/CVF International Conference on Computer Vision (ICCV)*, pages 90–101, 2023. 2
- [66] Zhixia Zhang, Zixuan Huang, Xin Xia, Deqing Wang, Fuzhen Zhuang, Shuai Ma, Ning Ding, Yaodong Yang, Jianxin Li, and Yikun Ban. Heterogeneous agent collaborative reinforcement learning, 2026. 13
- [67] Chujie Zheng, Kai Dang, Bowen Yu, Mingze Li, Huiqiang Jiang, Junrong Lin, Yuqiong Liu, Hao Lin, Chencan Wu, Feng Hu, An Yang, Jingren Zhou, and Junyang Lin. Stabilizing reinforcement learning with llms: Formulation and practices, 2025.
- [68] Chujie Zheng, Shixuan Liu, Mingze Li, Xiong-Hui Chen, Bowen Yu, Chang Gao, Kai Dang, Yuqiong Liu, Rui Men, An Yang, Jingren Zhou, and Junyang Lin. Group sequence policy optimization, 2025. 13
- [69] Yaozong Zheng, Bineng Zhong, Qihua Liang, Zhiyi Mo, Shengping Zhang, and Xianxian Li. Odtrack: Online dense temporal token learning for visual tracking. *Proceedings of the AAAI Conference on Artificial Intelligence*, 38(7):7588–7596, 2024. 1, 2, 3, 5, 6, 7, 14
- [70] Kaiyang Zhou, Jingkang Yang, Chen Change Loy, and Ziwei Liu. Learning to prompt for vision-language models. *International Journal of Computer Vision*, 130(9):2337–2348, 2022. 3